





Development of High-Power Charge Pump Rectifier for Microwave Wireless Power Transmission

KOKI MIWATASHI ¹, TAKASHI HIRAKAWA ² (Member, IEEE),
NAOKI SHINOHARA ³ (Senior Member, IEEE), AND TOMOHIKO MITANI ³ (Member, IEEE)
(Regular Paper)

¹Sony Semiconductor Solutions Corporation, Kanagawa 243-0014, Japan

²Softbank Corp., Aomi, Koto-ku, Tokyo 135-0064, Japan

³Research Institute for Sustainable Humanosphere, Kyoto University, Uji, Kyoto 611-0011, Japan

CORRESPONDING AUTHOR: Koki Miwatashi (e-mail: miwatashikoki@yahoo.co.jp).

ABSTRACT This study theoretically and experimentally indicates that a charge pump rectifier for low-power rectifiers such as RF-ID can be applied to high-power rectifiers and can attain the same level of RF-dc conversion efficiency and twice as high power rectification as the single-shunt rectifiers. A high-power rectifier is primarily a single-shunt rectifier, and a charge pump rectifier that applies twice the output voltage is used in low-power applications such as RF-ID. We aim to enhance the power of charge pump rectifiers by focusing on their characteristics. A fabricated 5.8 GHz charge pump rectifier achieved an RF-dc conversion efficiency of 70.8% at an input power of 8.0 W and a load resistance of 150 Ω . This result is also the highest efficiency for 39 dBm rectifiers in the 5.8 GHz band. Compared to a single-shunt rectifier with the same diode, the charge pump rectifier generated twice the input power and efficiency difference of 2.9% at the maximum input power. These results indicate that the charge pump rectifier has an advantage over the single-shunt rectifier in high-power rectifiers.

INDEX TERMS Rectifiers, RF circuits, Schottky diodes, wireless power transmission, circuit theory.

I. INTRODUCTION

Wireless power transmission (WPT) is an innovative technology that is becoming more commercialized. N. Tesla proposed WPT at the beginning of the 20th century, and it has been studied for over 100 years [1]. In recent years, WPT has been put to practical use in charging electric vehicles and smartphones [2], [3]. The microwave wireless power transmission (MWPT) has been the subject of several experiments since W.C. Brown's experiment in 1964 [4], [5]. MWPT technology is expected to be used in space solar power satellites, drones, and supplying power to buildings that are inaccessible because of disasters [6], [7], [8]. The system consists of signal generators, amplifiers, transmitting and receiving antennas, rectifiers, and output loads, and the total efficiency of these components is the final transmission efficiency. The efficiency of the rectifiers, which converts received radio waves into

dc power, is an important factor in improving the MWPT system's efficiency. The diodes must have low parasitic resistance, junction capacitance, threshold voltage, and high breakdown voltage for RF-dc conversion efficiency [9]. In addition, the higher the input power, the greater the chance of diode damage from the heat generated by the diode current. There is a limit to the diode's breakdown voltage; hence, the input power is also limited. In MWPT with high frequency, the diodes must operate at high speed. Therefore, it is difficult to develop diodes that can generate both high power and efficiency. For example, rectifiers using GaAs Schottky barrier diodes have achieved a high efficiency of 91% at 5 W input power, but the basic frequency is 2.45 GHz [10]. At 5.8 GHz, the rectifier with a Si Schottky Barrier Diode (SBD) has an efficiency of 82% with 50 mW input power, whereas the one with a GaAs SBD (MA4E1317) has an efficiency of 82.7%

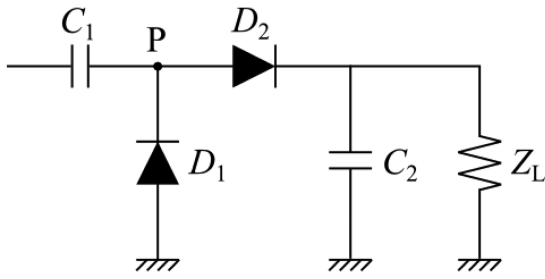


FIGURE 1. Schematic of an ideal charge pump rectifier.

with 49.09 mW [11], [12]. Furthermore, the development of Schottky barrier diodes with GaN, a power semiconductor, have progressed in recent years, and a rectifier with a GaN diode has achieved an efficiency of 71% at 2.5 W input power and 50% at 6.4 W input power in 5.8 GHz [13]. These circuits are single-shunt rectifiers with a single diode. This circuit type is fundamental at high frequencies and commonly used in rectifiers for high-power applications.

The purpose of this study is to design a 10 W class high-power and high-efficiency rectifier for high power applications like EVs and drones. To design a high-power and high-efficiency rectifier, we focused on a charge pump rectifier, which is used in low-power. The charge pump rectifier has the characteristic of doubling the output voltage compared to the single-shunt rectifier. WPT for low-power applications, including energy harvesting and RF-ID, requires a high output voltage. The WPT is often taken advantage of this characteristics of charge pump rectifiers. This characteristic is synonymous with halving the output current. This characteristic indicates that the diode current in the charge pump rectifier can be reduced. In a previous publication, a 5.8 GHz class-F charge pump rectifier for a satellite's internal wireless system was designed and achieved an RF-dc conversion efficiency of 71% [14]. However, since this rectifier's input power is 30 mW, it cannot be used in high-power systems such as EVs and drones. Thus, in this study, a high-power charge pump rectifier is proposed, and its advantage over a single-shunt rectifier is investigated in terms of efficiency and power.

II. THEORETICAL ANALYSIS FOR CHARGE PUMP RECTIFIER

In this section, the theoretical operation of an ideal charge pump rectifier is explained. It is also compared with a single-shunt rectifier. The single-shunt rectifier's theoretical operation has already been investigated [15]. The operation of a charge pump rectifier is analyzed in the same method.

A. OPERATION OF AN IDEAL CHARGE PUMP RECTIFIER

Fig. 1 shows a schematic of an ideal charge pump rectifier. This charge pump rectifier is solved using a distributed constant circuit. The diodes, D_1 and D_2 , in the charge pump rectifier are considered to have ideal I – V characteristics, as shown in Fig. 2.

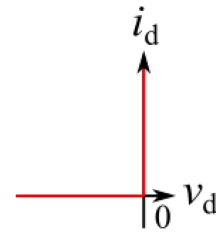


FIGURE 2. I – V characteristics of the diodes in the charge pump rectifier.

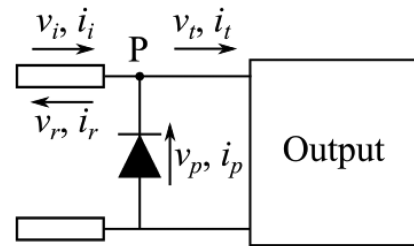


FIGURE 3. Circuit around point P in the charge pump rectifier.

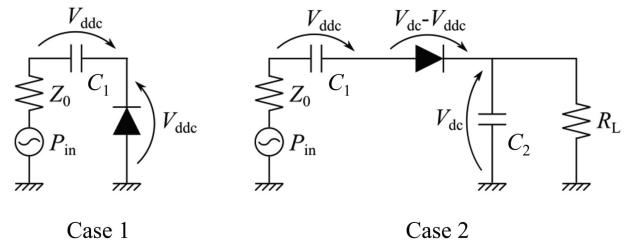


FIGURE 4. Two paths in an ideal charge pump rectifier.

First, we consider the point (P) between D_1 and D_2 . Fig. 3 shows the circuit around point P. Considering incident, reflection, and transmission waves in Fig. 3, the boundary conditions at point P are given by (1)–(4) from Kirchoff's and Ohm's law. The capacitor (C_2) on the output side should be large enough to act as an RF short.

$$v_i + v_r = v_p = v_t \quad (1)$$

$$i_i + i_r = -i_p + i_t \quad (2)$$

$$i_i = \frac{1}{Z_0} v_i, \quad i_r = -\frac{1}{Z_0} v_r \quad (3)$$

$$i_p = f(v_p), \quad i_t = g(v_t) \quad (4)$$

Equation (4) indicates that i_p and i_t are the functions of v_p and v_t respectively. The characteristics of $i_p - v_p$ and $i_t - v_t$ are the relationship of Fig. 2 because D_1 and D_2 are the ideal diodes. Equations (2) and (3) derives the following ones.

$$v_t = 0, \quad i_t = \frac{2}{Z_0} v_i, \quad v_p = 0, \quad i_p = 0 \quad (v_i \geq 0) \quad (5)$$

$$v_p = 0, \quad i_p = -\frac{2}{Z_0} v_i, \quad v_t = 0, \quad i_t = 0 \quad (v_i \leq 0) \quad (6)$$

Next, we consider the dc voltages of the diodes. We consider each case of the two paths as shown in Fig. 4 with the

dc voltages. First, we consider the path as shown on Case 1 of Fig. 4. With the dc voltage (V_{ddc}) of C_1 , (1) becomes (7).

$$v_i + v_r = v_p - V_{\text{ddc}} \quad (7)$$

On the other hand, (2)–(4) are the same as the dc voltages. Equations (5) and (6) are changed to (9).

$$v_p = v_i + v_r + V_{\text{ddc}}, \quad i_p = 0 \quad (v_i + V_{\text{ddc}} \geq 0) \quad (8)$$

$$v_p = 0, \quad i_p = -\frac{1}{Z_0}(2v_i + V_{\text{ddc}}) + i_t \quad (v_i + V_{\text{ddc}} \leq 0) \quad (9)$$

Second, we consider the path shown on Case 2 of Fig. 4. Equations (11) and (12) can be obtained by considering the dc voltage (V_{dc}) of C_2 and V_{ddc} .

$$v_i + v_r = v_t + V_{\text{dc}} - V_{\text{ddc}} = v_p - V_{\text{ddc}} \quad (10)$$

$$v_t = 0, \quad i_t = \frac{1}{Z_0}(2v_i + V_{\text{ddc}} - V_{\text{dc}}) + i_p \quad (v_i + V_{\text{ddc}} - V_{\text{dc}} \geq 0) \quad (11)$$

$$v_t = -(v_i + v_r) - V_{\text{ddc}} + V_{\text{dc}}, \quad i_t = 0 \quad (v_i + V_{\text{ddc}} - V_{\text{dc}} \leq 0) \quad (12)$$

By symmetry, the dc voltage of D_2 is the same as that of D_1 .

$$V_{\text{ddc}} = V_{\text{dc}} - V_{\text{ddc}} \quad (13)$$

$$V_{\text{dc}} = 2V_{\text{ddc}} \quad (14)$$

Changing V_{ddc} with V_{dc} in (8)–(12), (15)–(17) are obtained.

$$v_p = 0, \quad i_p = -\frac{1}{Z_0}\left(2v_i + \frac{1}{2}V_{\text{dc}}\right), \quad (15)$$

$$v_t = -(v_i + v_r) + \frac{1}{2}V_{\text{dc}}, \quad i_t = 0 \quad \left(v_i \leq -\frac{1}{2}V_{\text{dc}}\right)$$

$$v_p = v_i + v_r + \frac{1}{2}V_{\text{dc}}, \quad i_p = 0, \quad (16)$$

$$v_t = -(v_i + v_r) + \frac{1}{2}V_{\text{dc}}, \quad i_t = 0 \quad \left(-\frac{1}{2}V_{\text{dc}} \leq v_i \leq \frac{1}{2}V_{\text{dc}}\right)$$

$$v_p = v_i + v_r + \frac{1}{2}V_{\text{dc}}, \quad i_p = 0, \quad (17)$$

$$v_t = 0, \quad i_t = \frac{1}{Z_0}\left(2v_i - \frac{1}{2}V_{\text{dc}}\right) \quad \left(\frac{1}{2}V_{\text{dc}} \leq v_i\right)$$

When the incident wave is negative, the incident and reflected waves are as shown in the upper part of Fig. 5. However, when the incident wave is positive, the incident and reflected waves are shown in the lower part of Fig. 5.

The diode voltages and currents in the steady state can be represented in Fig. 6 using these results. V_{in} indicates the amplitude of v_i . Fig. 7 shows the diode voltage and current in the ideal single-shunt rectifier. These figures show that the diode voltage has the same waveform and the diode current has exactly half the waveform compared to the single-shunt

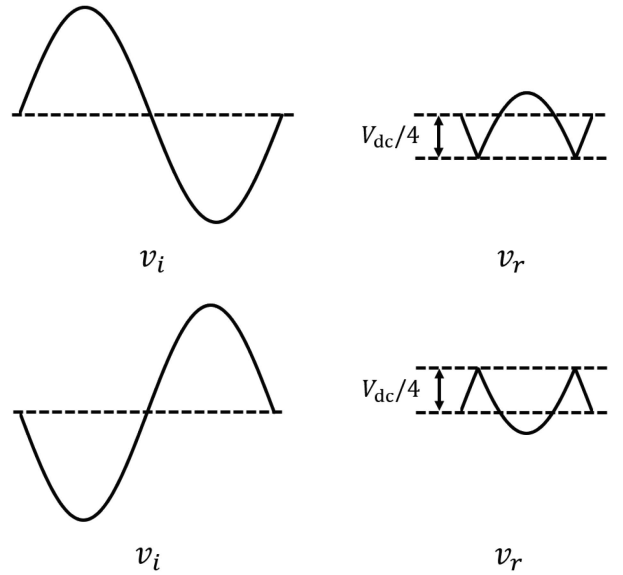


FIGURE 5. Incident and reflected waves at each time step.

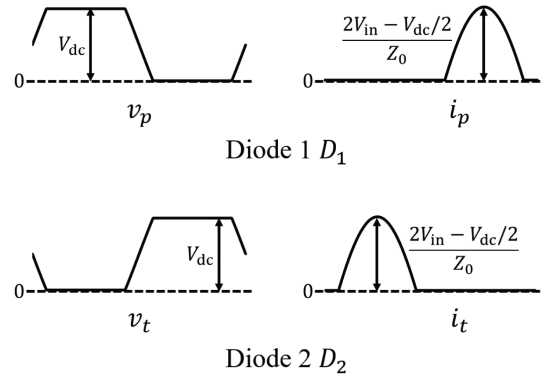


FIGURE 6. Waveforms of the two diodes in the ideal charge pump rectifier.

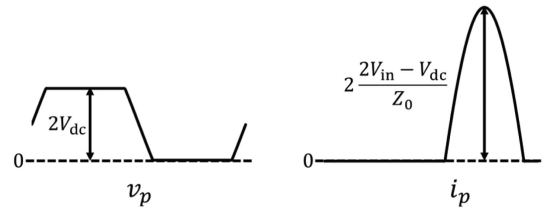


FIGURE 7. Waveforms of the diode in the ideal single-shunt rectifier.

rectifier because V_{dc} of the single-shunt rectifier is half that of the charge pump rectifier. These results indicate that the charge pump rectifier is effective at high power because the power in the single diode is halved compared to the single-shunt rectifier.

The next step is to calculate the ideal maximum RF-dc conversion efficiency of the charge pump rectifier. The average current of the diodes in a steady state can be expressed using

the following equation:

$$\bar{i}_p = \frac{1}{\pi} \int_{\arcsin\left(\frac{V_{dc}}{4V_{in}}\right)}^{\frac{\pi}{2}} \frac{2}{Z_0} \left(V_{in} \sin\theta - \frac{V_{dc}}{4} \right) d\theta = I_{dc} \quad (18)$$

$$V_{dc} = \frac{2Z_L}{\pi Z_0} \int_{\arcsin\left(\frac{V_{dc}}{4V_{in}}\right)}^{\frac{\pi}{2}} \frac{2}{Z_0} \left(V_{in} \sin\theta - \frac{V_{dc}}{4} \right) d\theta. \quad (19)$$

V_{dc} is equal to output voltage V_{out} from Fig. 4. The input power P_{in} and the output power P_{out} are indicated as (20)–(21) with V_{in} , V_{out} , Z_0 and R_L .

$$P_{in} = \frac{V_{in}^2}{2Z_0} \quad (20)$$

$$P_{out} = \frac{V_{out}^2}{R_L} \quad (21)$$

Normalizing as the following (22)–(25), (26) can be derived from (19).

$$\hat{V} = \frac{V_{out}}{V_{in}} \quad (22)$$

$$\hat{Z} = \frac{R_L}{Z_0} \quad (23)$$

$$\hat{I} = \frac{\hat{V}}{\hat{Z}} \quad (24)$$

$$\eta_{dc} = \frac{P_{out}}{P_{in}} = \frac{2\hat{V}^2}{\hat{Z}} = 2\hat{I}^2\hat{Z} = 2\hat{I}\hat{V} \quad (25)$$

$$\frac{2}{\pi} \sqrt{1 - \frac{\hat{V}^2}{16}} + \frac{1}{2\pi} \hat{V} \arcsin\left(\frac{\hat{V}}{4}\right) - \frac{\hat{V}}{4} = \frac{\hat{V}}{\hat{Z}} \quad (26)$$

According to [15], the ideal single-shunt rectifier has the following (27).

$$\frac{4}{\pi} \sqrt{1 - \frac{\hat{V}^2}{4}} + \frac{2}{\pi} \hat{V} \arcsin\left(\frac{\hat{V}}{2}\right) - \hat{V} = \frac{\hat{V}}{\hat{Z}} \quad (27)$$

When $\hat{V} = \hat{V}/2$ and $\hat{I} = 2\hat{I}$ are substituted, (26) equals (27). This result shows that the charge pump rectifier doubles the output voltage and halves the output current when compared to the single-shunt rectifier. Furthermore, Fig. 8, which is the numerical results of (26) and (27), shows that the RF-dc conversion efficiency, η_{dc} , in both rectifiers is 92.26%, and the optimal load resistance curve of the charge pump rectifier is shifted four times to the right compared to that of the single-shunt rectifier.

When the input power is increased to n times, the diode voltage and current are increased \sqrt{n} times. Thus, the diode voltage of the charge pump rectifier exceeds that of the single-shunt rectifier, and this circuit cannot achieve high power by charge pump rectifiers. In the next section, we increased the rectification power of a charge pump rectifier by adding a matching circuit.

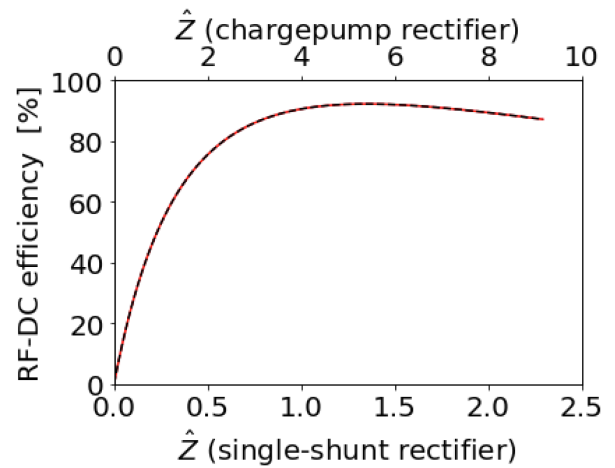


FIGURE 8. Relationship between RF-dc conversion efficiencies and the normalization load resistances in the ideal charge pump rectifier and the ideal single-shunt rectifier.

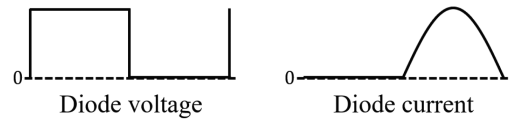


FIGURE 9. Diode waveforms of an ideal single-shunt rectifier.

B. SIMULATIONS OF IDEAL CHARGE PUMP AND SINGLE-SHUNT RECTIFIERS WITH MATCHING CIRCUITS FOR HIGH-POWER

Next, we analyze the charge pump rectifier and the single-shunt rectifier with the matching circuit and compare the efficiencies of the two rectifiers. The matching circuit lowers the rectifier's impedance, resulting in higher rectifier power.

1) THEORY OF AN IDEAL CHARGE PUMP RECTIFIER WITH AN IDEAL MATCHING CIRCUIT

A single-shunt rectifier can get a reflection power of 0% and an RF-dc conversion efficiency of 100% if its matching circuit processes all the diode's harmonics [16]. Fig. 9 shows the diode's theoretical voltage and current waveforms at that time. The shape of the diode waveforms is the current waveform to half-sine wave and the voltage waveform to a square wave, which are represented by (28) and (29).

$$v_d = \begin{cases} V_d & (0 \leq \omega t < \pi), \\ 0 & (\pi \leq \omega t < 2\pi). \end{cases} \quad (28)$$

$$i_d = \begin{cases} 0 & (0 \leq \omega t < \pi), \\ I_d \sin\omega t & (\pi \leq \omega t < 2\pi). \end{cases} \quad (29)$$

In the ideal rectifier with a matching circuit, the output voltage V_{out} , current I_{out} , load resistance R_L , and input power P_{in} are expressed with a period $T (= 2\pi/\omega)$ by (30)–(33) since the RF-dc conversion efficiency is 100%.

$$V_{out} = \frac{1}{T} \int_0^T v_d dt = \frac{1}{2} V_d \quad (30)$$

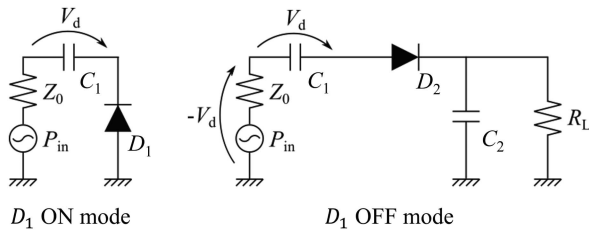


FIGURE 10. Operation of the ideal charge pump rectifier at the ON and OFF modes of D_1 .

$$I_{out} = \frac{1}{T} \int_0^T i_d dt = \frac{1}{\pi} I_d \quad (31)$$

$$R_L = \frac{V_{out}}{I_{out}} = \frac{\pi V_d}{2I_d} \quad (32)$$

$$P_{in} = V_{out} I_{out} = \frac{V_d I_d}{2\pi} \quad (33)$$

Next, we assume the same conditions for the charge pump rectifier. From Section II-A, when diode D_1 is in ON mode, D_2 is in OFF mode. Assuming the same diode operation, as in the single-shunt rectifier, V_d is applied to the capacitor C_1 as shown in Fig. 10. By contrast, when D_1 is in ON mode, D_2 is in OFF mode. Equations (34)–(37) can be derived from the V_d of C_1 and the voltage and current of D_2 as in Fig. 10.

$$V_{out} = \frac{1}{T} \int_0^T 2v_d dt = V_d \quad (34)$$

$$I_{out} = \frac{1}{T} \int_0^T i_d dt = \frac{1}{\pi} I_d \quad (35)$$

$$R_L = \frac{V_{out}}{I_{out}} = \frac{\pi V_d}{I_d} \quad (36)$$

$$P_{in} = V_{out} I_{out} = \frac{V_d I_d}{\pi} \quad (37)$$

These equations indicate that the input power and load resistance of the charge pump rectifier are both twice as high as those of the single-shunt rectifier.

2) SIMULATIONS OF THE IDEAL CHARGE PUMP RECTIFIER WITH THE MATCHING CIRCUIT

Next, we verify the theory using a circuit analysis simulation. In this analysis, we use Keysight’s Advanced Design System (ADS) to analyze the circuits shown in Figs. 11 and 12. The rectifier’s diodes should operate ideally, but the circuit in the ideal diode cannot be analyzed using the harmonic balance method in ADS. Therefore, we use the diode with the parameters in Table 1, which allows for an ideal operation as much as possible. The single-shunt rectifier’s input power is 10 W, which is large enough to reduce the effect of the diode’s threshold voltage. The load resistance is 100 Ω for no particular reason. The input power and load resistance of the charge pump rectifier are 20 W and 200 Ω , respectively, which is double those of the single-shunt rectifier. The basic frequency and characteristic impedance of the two rectifiers

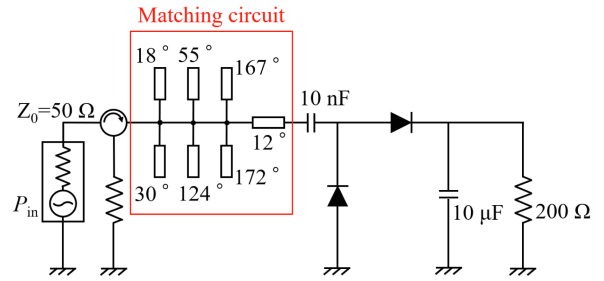


FIGURE 11. Schematic of an ideal charge pump rectifier with an optimized matching circuit.

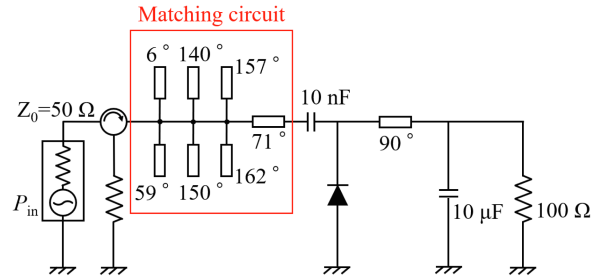


FIGURE 12. Schematic of an ideal single-shunt rectifier with an optimized matching circuit.

TABLE 1. SPICE Parameters of the Diode in the Two Rectifiers

Parameters	
Saturation Current, I_S	$1.0e^{-14} \mu A$
Series Resistance, R_s	0 Ω
Emission Coefficient, N	0.01
Breakdown Voltage, B_v	∞ V
Zero-Bias Junction Capacitance, C_{j0}	0.0 F
Junction Grading Coefficient, M	0.5
Junction Potential, V_j	0 V

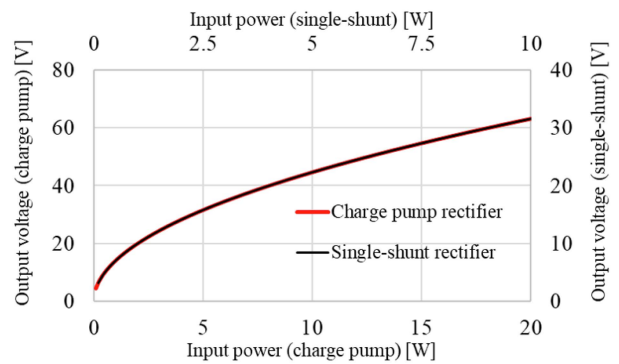


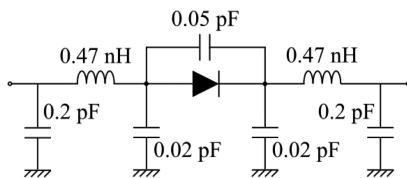
FIGURE 13. Relationship between output voltage and input power of the two simulated rectifiers.

are 1 GHz and 50 Ω , respectively. The matching circuits of the two rectifiers consist of one lossless transmission line and six stubs for sufficient harmonic processing, and they are randomly optimized for 100% of RF-dc conversion efficiency.

Both of the rectifiers have 99.9% RF-dc conversion efficiency, which is approximately 100%. Fig. 13 shows the

TABLE 2. SPICE Parameters of the GaAs Schottky Barrier Diode in the Single-Shunt Rectifier and Charge Pump Rectifier

Parameters	
Saturation Current, I_S	8.41 μA
Series Resistance, R_s	0.7 Ω
Emission Coefficient, N	1.16
Breakdown Voltage, B_v	60 V
Zero-Bias Junction Capacitance, C_{j0}	3.2 pF
Junction Grading Coefficient, M	0.53
Junction Potential, V_j	0.84 V

**FIGURE 14.** Equivalent circuit of the diode package SOD-523.

output voltage with sweeping input power. The charge pump rectifier's $V - P$ curve is identical to the single-shunt rectifier's $V - P$ curve when enlarged twice. By doubling the input power and load resistance, the diodes of the charge pump and single-shunt rectifiers perform an equivalent operation. Furthermore, the two efficiencies at this time are essentially equal. This result shows that the charge pump rectifier has an equivalent rectifying capability and can increase power by two times when compared to the single-shunt rectifier. This means that the charge pump rectifier is superior to the single-shunt rectifier in high power. Moreover, in the design of the charge pump rectifier, the diodes operate similarly to those in the single-shunt rectifier by making the load resistance twice as large as that of the single-shunt rectifier. In the next section, we design and fabricate the charge pump rectifier. Then, by comparing the charge pump rectifier to the single-shunt rectifier, we verify the former's advantage.

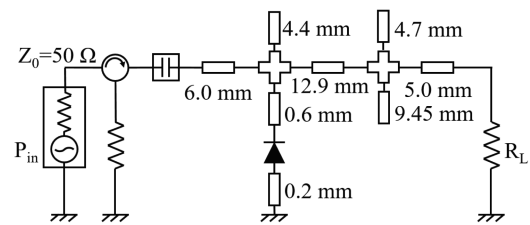
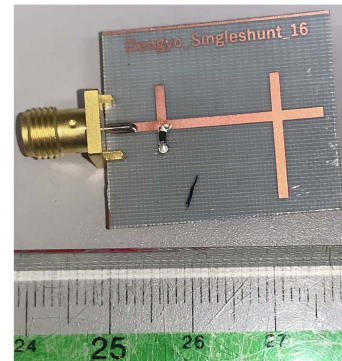
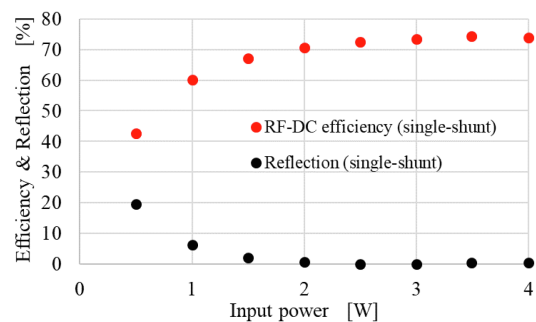
III. DESIGN OF A HIGH-POWER CHARGE PUMP RECTIFIER

RECTIFIER

In this section, we will design single-shunt and charge pump rectifiers. The design was done using Keysight's ADS. The diode to be used is a GaAs Schottky barrier diode with the SPICE parameters listed in Table 2. The package of this diode is SOD-523, and the equivalent circuit model for the package is the one shown in Fig. 14.

A. DESIGN OF A SINGLE-SHUNT RECTIFIER

In this section, we design and compare a single-shunt rectifier. Fig. 15 shows the designed rectifier. The output filter is a class-F filter that processes even-order and second-order harmonics. To achieve the maximum RF-dc conversion efficiency, the rectifier is designed for a continuous wave at 5.8 GHz with an input power of 5 W. The rectifier's substrate has the dielectric constant of 2.16, a dissipation factor of 0.0004, and a nominal thickness of 0.4 mm. Microstrip lines were selected as transmission lines, and the width of the lines

**FIGURE 15.** Schematic of the designed single-shunt rectifier.**FIGURE 16.** Fabricated single-shunt rectifier.**FIGURE 17.** Relationship between RF-dc conversion efficiency and input power of the fabricated single-shunt rectifier.

was set to 1.15 mm to achieve a characteristic impedance of 50 Ω .

Fig. 15 shows the designed single-shunt rectifier, and Fig. 16 shows the fabricated rectifier. Fig. 17 shows the $\eta - P_{in}$ characteristics of the fabricated rectifier. The maximum RF-dc conversion efficiency in this circuit was 74.8% at an input power of 3.5 W and a load resistance of 70 Ω . When the circuit was supplied an input power of over 4 W, the temperature of the diodes instantly increased, and the rectifier failed. The diode's thermal runaway caused this phenomenon. In addition, the maximum input power in this circuit was 4.0 W with an RF-dc conversion efficiency of 73.7% and a load resistance of 70 Ω . The circuit's size is 2.5 mm \times 2.9 mm, and the dc power per unit area is 406.7 mW/mm².

B. DESIGN OF A CHARGE PUMP RECTIFIER

Next, we design a charge pump rectifier. Based on the design results of the single-shunt rectifier in Section III-A and the

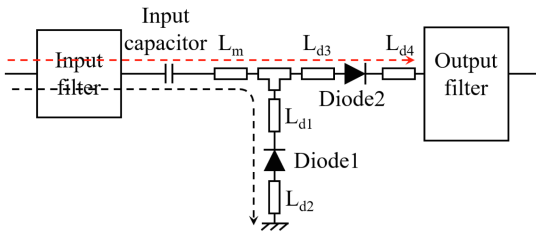


FIGURE 18. Positive and negative paths of the input wave to D_1 and D_2 .

analysis results in Section II-B, we estimated that the maximum input power of the charge pump rectifier using the diode with the SPICE parameters of Table 2 is 8.0 W. Based on the optimal load resistance obtained in the single-shunt rectifier, we designed the charge pump rectifier where the diode should perform the same operation under the conditions of twice the load resistance.

1) DESIGN OF AN OUTPUT FILTER

A charge pump rectifier with a class-F load was proposed by [14] for the rectifier's design at 5.8 GHz. This study proposes an output filter with open stubs of 90° and 45° behind diode D_2 . The smoothing capacitor of the charge pump rectifier makes the impedance of the output filter of zero at the harmonics generated by the diode. The $\lambda_n/4$ open stubs inserted instead of the smoothing capacitor can process these harmonics. Therefore, in this study, we designed the output filter with only $\lambda_1/4$ and $\lambda_2/4$ open stubs. This filter can process the fundamentals and harmonics up to the third order.

2) DESIGN OF AN INPUT AND MATCHING FILTERS

In designing high-power charge pump rectifiers, it is necessary to operate diodes 1 and 2 (D_1 and D_2 , respectively) just below their breakdown voltage and allowable current. This enhances the power capacity of the charge pump rectifier. In the charge pump rectifier, the transmission lines L_{d1} to L_{d4} shown in Fig. 18 are used for matching. In this case, considering the path of the input wave to D_1 and D_2 , the positive input wave passes through the red dashed line, and the negative input wave passes through the black dashed line in Fig. 18. This means that the input impedance, voltage, and current at the ON mode of D_1 and D_2 are equal using the relationship shown in (38).

$$L_{d1} = L_{d3}, \quad L_{d2} = L_{d4} \quad (38)$$

We designed the input filter and matching circuit under the conditions of (38).

3) DESIGN OF THE WHOLE CHARGE PUMP RECTIFIER

The charge pump rectifier was designed based on Sections III-B III-B1) and III-B2). Fig. 19 shows the designed circuit. The front stage input filter, the matching circuit before and after the diodes, and the backstage output filter make up the circuit. The basic wave is a continuous wave at 5.8 GHz, with the same substrate and line width as in Section III-A. The circuit

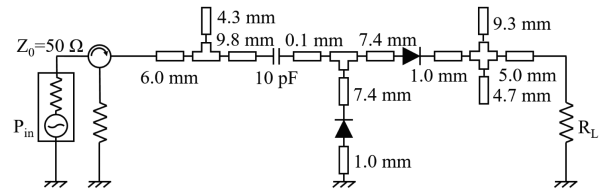


FIGURE 19. Designed charge pump rectifier.

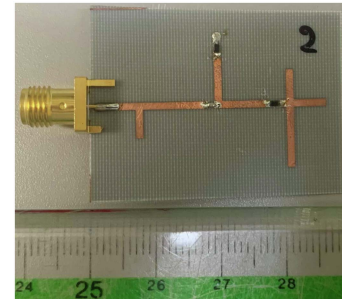


FIGURE 20. Fabricated charge pump rectifier.

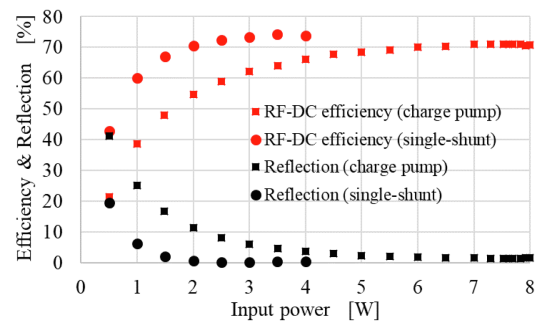


FIGURE 21. Relationship between RF-dc conversion efficiencies and input power of the two fabricated rectifiers.

was matched to achieve the maximum RF-dc conversion efficiency at the input power of 8.0 W.

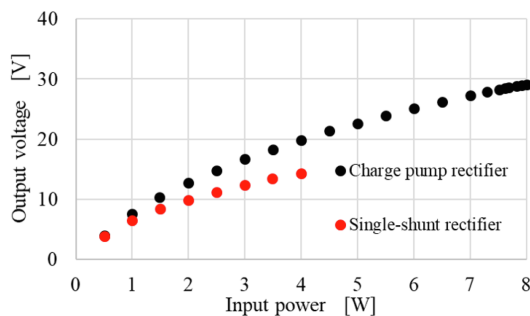
IV. EXPERIMENTAL RESULTS OF THE CHARGE PUMP RECTIFIER AND COMPARISON WITH THE SINGLE-SHUNT RECTIFIER

Fig. 20 shows the fabricated charge pump rectifier. Fig. 21 shows the measured $\eta - P_{in}$ characteristics of the fabricated single-shunt and charge pump rectifiers. The maximum RF-dc conversion efficiency of 71.1% in the charge pump rectifier is practically the same level as that in the single-shunt rectifier. At the same time, the input power is 7.69 W, and the load resistance is 150Ω . The maximum input power of the charge pump rectifier is 8.0 W with an RF-dc conversion efficiency of 70.8%. This rectifier has the highest efficiency for 39 dBm rectifiers in the 5.8 GHz band, as shown in Table 3 [11], [12], [13], [17], [18].

When the maximum input power of the charge pump rectifier and the single-shunt rectifier were compared, the charge pump rectifier was twice as powerful. In addition, its optimal load resistance is 150Ω , which is about 2.1 times that of

TABLE 3. Comparison of Some 5.8 GHz High-Efficiency Rectifiers

Papers	Diode Types	Rectifier Types	Input Power	RF-dc
[11]	Si SBD	Single-Shunt	50 mW	82 %
[12]	GaAs SBD	Single-Shunt	49.09 mW	82.7 %
[13]	GaN SBD	Single-Shunt	2.5 W	71 %
[13]	GaN SBD	Single-shunt	6.4 W	50 %
[17]	GaAs SBD	Single-Shunt	0.50 W	77.2 %
[18]	GaN HEMT	Single-Shunt	26.3 W	44.8 %
This Work	GaAs SBD	Charge Pump	7.69 W	71.1 %
This Work	GaAs SBD	Charge Pump	8.0 W	70.8 %

**FIGURE 22. Output voltages versus the input powers of the two fabricated rectifiers.****FIGURE 23. Temperature profile of the two diodes of the fabricated charge pump rectifier.**

the single-shunt rectifier. Fig. 22 shows the $V_{\text{out}} - P_{\text{in}}$ characteristics of the two rectifiers. The charge pump rectifier's $V - P$ curve was almost identical to the single-shunt rectifier's $V - P$ curve when enlarged twice. Furthermore, we measured the temperature of the diodes in order to visualize the power delivered to the diodes. The result is shown in Fig. 23, and the temperatures of these two diodes are almost the same. The result indicates that similar power is delivered to these diodes, which results in heat due to similar diode losses. These results are almost proven to be practically the same as the simulation results in Section II-B. Furthermore, the circuit size of the charge pump rectifier was $2.9 \text{ mm} \times 3.9 \text{ mm}$, which was 1.56 times larger than that of the single-shunt rectifier. Thus, the rectification power per unit area was $501 \text{ mW}/\text{mm}^2$, which is

1.23 times larger than that of the single-shunt rectifier. These results indicate that a charge pump rectifier is preferable to a single-shunt rectifier for high-power rectifiers.

V. CONCLUSION

In this study, the advantage of charge pump rectifiers in high-power rectifiers was theoretically and experimentally investigated. At an input power of 7.69 W and a load resistance of 150Ω , the fabricated charge pump rectifier achieved a maximum RF-dc conversion efficiency of 71.1%. This result is also the highest efficiency for 39 dBm rectifiers in the 5.8 GHz band. The fabricated charge pump rectifier achieved an RF-dc conversion efficiency of 70.8% at an input power of 8.0 W and a load resistance of 150Ω , which is practically the same efficiency as that of the single-shunt rectifier using the same diode. Furthermore, the maximum input power of the charge pump rectifier was twice that of the single shunt rectifier. These results show that the charge pump rectifier has an advantage over the single-shunt rectifier for high-power rectifiers.

REFERENCES

- [1] N. Tesla, "Experiments with alternate currents of high potential and high frequency," *Trans. Amer. Inst. Elect. Eng.*, vol. 8, no. 1, pp. 266–319, 1891.
- [2] N. Shinohara, "Wireless power transmission progress for electric vehicle in Japan," in *Proc. IEEE Radio Wireless Symp.*, 2013, pp. 109–111.
- [3] [Online]. Available: <https://qi-wireless-charging.net/qi-enabled-phones/>
- [4] W. Brown, "Experiments in the transportation of energy by microwave beam," *IRE Int. Conv. Rec.*, vol. 12, pp. 8–17, 1964.
- [5] N. Shinohara, "Beam control technologies with a high-efficiency phased array for microwave power transmission in Japan," *Proc. IEEE*, vol. 101, no. 6, pp. 1448–1463, Jun. 2013.
- [6] W. C. Brown, "The history of power transmission by radio waves," *IEEE Trans. Microw. Theory Techn.*, vol. 32, no. 9, pp. 1230–1242, Sep. 1984.
- [7] N. Shinohara, "Novel beam-forming technology for WPT system to flying drone," in *Proc. IEEE Wireless Power Transfer Conf.*, 2020, pp. 9–12.
- [8] C.-H. Lee, "Wireless information and power transfer for communication recovery in disaster areas," in *Proc. IEEE Int. Symp. World Wireless, Mobile Multimedia Netw.*, 2014, pp. 1–4.
- [9] T.-W. Yoo and K. Chang, "Theoretical and experimental development of 10 and 35GHz rectennas," *IEEE Trans. Microw. Theory Techn.*, vol. 40, no. 6, pp. 1259–1266, Jun. 1992.
- [10] C. Wang, B. Yang, and N. Shinohara, "Study and design of a 2.45-GHz rectifier achieving 91% efficiency at 5-W input power," *IEEE Microw. Wireless Compon. Lett.*, vol. 31, no. 1, pp. 76–79, Jan. 2021.
- [11] J.O. McSpadden, L. Fan, and K. Chang, "Design and experiments of a high-conversion-efficiency 5.8-GHz rectenna," *IEEE Trans. Microw. Theory Techn.*, vol. 46, no. 12, pp. 2053–2060, Dec. 1998.
- [12] Y.-Ho Suh and K. Chang, "A novel dual frequency rectenna for high efficiency wireless power transmission at 2.45 and 5.8 GHz," in *IEEE MTT-S Int. Microw. Symp. Dig.*, 2002, vol. 2, pp. 1297–1300.
- [13] K. Dang et al., "A 5.8-GHz high-power and high-efficiency rectifier circuit with lateral GaN Schottky diode for wireless power transfer," *IEEE Trans. Power Electron.*, vol. 35, no. 3, pp. 2247–2252, Mar. 2020.
- [14] C. Wang, N. Shinohara, and T. Mitani, "Study on 5.8-GHz single-stage charge pump rectifier for internal wireless system of satellite," *IEEE Trans. Microw. Theory Techn.*, vol. 65, no. 4, pp. 1058–1065, Apr. 2017.

- [15] T. Hirakawa and N. Shinohara, "Theoretical analysis and novel simulation for single shunt rectifiers," *IEEE Access*, vol. 9, pp. 16615–16622, 2021.
- [16] J. Guo, H. Zhang, and X. Zhu, "Theoretical analysis of RF-DC conversion efficiency for class-F rectifiers," *IEEE Trans. Microw. Theory Techn.*, vol. 62, no. 4, pp. 977–985, Apr. 2014.
- [17] T. Tanaka et al., "High breakdown voltage GaAs Schottky diode for a high efficiency rectifier in microwave power transmission systems," in *Proc. IEEE Int. Symp. Radio-Freq. Integration Technol.*, 2015, pp. 199–201.
- [18] S. Yoshida, K. Nishikawa, and S. Kawasaki, "10 W class high power C-band rectifier using GaN HEMT," in *Proc. IEEE Wireless Power Transfer Conf.*, 2019, pp. 595–598.



KOKI MIWATASHI received the B.E. degree in electrical and electronic engineering and the M.E. degree in electrical engineering from Kyoto University, Kyoto, Japan, in 2020 and 2022, respectively. He is now an engineer at Sony Semiconductor Solutions Corporation, Kanagawa, Japan.



TAKASHI HIRAKAWA (Member, IEEE) received the B.E. degree in electrical engineering and the M.E. and Ph.D (Eng.) degrees in electrical engineering from Kyoto University, Kyoto, Japan, in 2016, 2018, and 2021, respectively. His research focuses on characteristics of high-frequency rectifiers. He is currently a Researcher at the System Design R&D Department, Technology Research Laboratory, SoftBank Corp., Tokyo, Japan. His current research interests include RF-input rectifiers and wireless power transfer system.



NAOKI SHINOHARA (Member, IEEE) received the B.E. degree in electronic engineering and the M.E. and Ph.D (Eng.) degrees in electrical engineering from Kyoto University, Kyoto, Japan, in 1991, 1993, and 1996, respectively. He was a Research Associate with Kyoto University in 1996. In 2010, he was a Professor with Kyoto University. He has been engaged in research on solar power station/satellite and microwave power transmission system. He was an IEEE MTT-S Distinguish Microwave Lecturer (2016–2018), and has been an

IEEE MTT-S AdCom Member since 2022. He was an IEEE MTT-S Technical Committee 25 (Wireless Power Transfer and Conversion) Former Chair, IEEE MTT-S MGA (Member Geographic Activities) Region 10 Regional Coordinator, IEEE WPT Initiative Member, IEEE MTT-S Kansai Chapter TPC Member, IEEE Wireless Power Transfer Conference founder and ExCom Committee Member, URSI Commission D Chair, *International Journal of Wireless Power Transfer* (Hindawi) Executive Editor, the First Chair and Technical Committee Member on IEICE Wireless Power Transfer, Japan Society of Electromagnetic Wave Energy Applications adviser, Space Solar Power Systems Society Vice Chair, Wireless Power Transfer Consortium for Practical Applications (WiPoT) chair, and Wireless Power Management Consortium (WPMc) Chair. His books are *Wireless Power Transfer via Radiowaves* (ISTE/Wiley), *Recent Wireless Power Transfer Technologies Via Radio Waves* (ed.) (River Publishers), and *Wireless Power Transfer: Theory, Technology, and Applications* (ed.) (IET), and some Japanese text books of WPT.



TOMOHIKO MITANI (Member, IEEE) received the B.E. degree in electrical and electronic engineering, the M.E. degree in informatics, and the Ph.D. degree in electrical engineering from Kyoto University, Kyoto, Japan, in 1999, 2001, and 2006, respectively. In 2003, he was an Assistant Professor with the Radio Science Center for Space and Atmosphere, Kyoto University. Since 2012, he has been an Associate Professor with the Research Institute for Sustainable Humanosphere, Kyoto University. His research interests include the

experimental study of magnetrons, microwave power transmission systems, and applied microwave engineering. Dr. Mitani is a member of the Institute of Electronics, Information and Communication Engineers and the Japan Society of Electromagnetic Wave Energy Applications. He has been a Board Member of JEMEA since 2015. He was the treasurer of IEEE MTT-S Kansai Chapter from 2014 to 2021, and has been Technical Committee Chair of the IEEE MTT-S Kansai Chapter since 2022.